JOURNAL OF MATERIALS SCIENCE 18 (1983) 2361–2370

Light induced ESR spectra in rutile powders

S. W. HODGSKISS, J. S. THORP, G. BROWN*
Department of Applied Physics and Electronics, University of Durham, UK

A series of rutile powders has been examined by electron spin resonance techniques before and after ultraviolet irradiaton at low temperatures. Prior to irradiation a broad line was seen at 4.2 K whose g-value ($g \approx 1.955$) was similar to that reported by Iyengar in hydrogen-reduced rutile. After ultraviolet irradiaton at 4.2 K a new line was observed. Computer simulation techniques showed that the best fit to the observed lineshape was obtained by taking $g_1 = g_2 = 2.0077$ and $g_3 = 2.015$ with Lorentzian broadening. Isochronal annealing of this centre showed marked decreases in the signal intensity at both 10 and 80 K; these are attributed, respectively, to thermal release of electrons from a shallow and a deep electron trap giving recombination at the centre.

1. Introduction

Unlike the abundant data from single crystal studies, there has been relatively little published literature concerning ESR analysis of rutile powders. In 1966, Iyengar [1] noted that the reduction of rutile powder in hydrogen gave rise to an asymmetric signal centred on $g \approx 1.96$, which was assigned to Ti^{3+} on normal cation sites. Later ESR techniques were used by Primet [2] in investigations of the surface chemistry of adsorbed gases.

ESR signals from powder samples are in general more difficult to interpret than their single crystal counterparts. Much of the valuable information which can be extracted by studying the angular variation of the spectrum is lost, since the component crystallites of a powder have random orientation with respect to the magnetic field. Thus, with anisotropic spectra the individual resonance lines from each crystallite are superimposed to give a much broader, usually asymmetric, powder absorption line. Very anisotropic single crystal spectra, such as those representing several of the impurity ions in rutile, may lead to powder signals which are so broad that they cannot be easily detected. It is sometimes possible, however, to extract some of the information needed to aid interpretation of powder spectra, by employing simulation techniques. This involves taking single crystal spin Hamiltonian parameters and using a computer program to generate a theoretical powder spectrum. The parameters may then be adjusted in order to alter the shape of the powder pattern, with the aim of reproducing the features of the experimental powder spectrum. This method has recently been adopted by Thorp and Eggleston [3] in studying the ESR powder spectra of Fe/TiO_2 and Cr/TiO_2.

A similar approach has been used here in a preliminary study of light-induced trapping centres in rutile powders. Rutile powders are widely used in paints and the occurrence and nature of trapping centres in them is a major factor influencing their degradation behaviour. In the work reported here the series of experimental powder-like samples examined contained different amounts of aluminium and had been subjected to various heat treatments during preparation; the primary aim was to examine the potential and sensitivity of ESR methods for monitoring the effects of small changes in composition.

2. Experimantal details

2.1. Sample composition

The seven rutile powder samples, which were supplied by Tioxide International Ltd., are listed in Table I. This shows that they comprised a 6-way factorial trial, with the aluminium concentration and the effect of an oxidizing heat treatment as the variables. Both parameters have a significant effect on the durability of paints made from these

*Present address: Marconi Avionics Ltd., Basildon, UK.

0022–2461/83 $03.00 + .12

TABLE I Aluminium concentrations, expressed as per cent alumina, and heat treatments of experimental rutile powders

Sample	Al_2O_3 (per cent)	Heat treatment
A	0.61	None
B	0.61	30 min at 600° C in O_2
C	3.28	None
D	3.28	30 min at 600° C in O_2
E	1.56	None
F	1.56	30 min at 600° C in O_2
G	1.56	30 min at 600° C in H_2

powders. The samples were submitted for ESR analysis with the hope that a centre could be identified whose concentration varied in a similar way to the paint durability. One of the powder samples (G) had been reduced by heating to 600° C in hydrogen for 30 min in order to provide a reference signal from intrinsic defects. A mass spectrographic analysis of the powders is presented in Table II. It should be noted that the concentrations of transition group ion impurities were relatively low, the major one, iron, being present only at between 25 and 35 ppm.

TABLE II Mass spectrographic analyses of powder samples; impurity concentrations given in ppm

Sample reference	A, B	C, D	E, F, G
Al_2O_3	6100	31 000	15 000
SiO_2	6000	6000	6000
MgO	6	20	12
P_2O_5	8	25	8
K_2O	4	5	2
CaO	10	15	8
V_2O_5	< 3	<3	<3
Cr_2O_3	<3	<3	<3
MnO	<3	<3	<3
Fe	25	35	25
NiO	⩽3	–	–
CoO	<3	<3	<3
Cu	<3	3	<3
ZnO	1	10	5
As_2O_3	35	4	1
SrO	<0.1	<0.1	<0.1
ZrO_2	15	20	2
Nb_2O_5	4	2	4
MoO_3	<3	<3	<3
Sn	13	4	4
Sb_2O_3	12	2	<1
BaO	0.5	0.5	<0.5
Ta_2O_5	1	3	5

2.2. ESR techniques

To obtain derivative spectra at 9 GHz both a Jeol and a Varian 4502-15 spectrometer were used, the latter proving particularly useful for cryogenic work and optical irradiation. Details of these facilities have been given by Hodgskiss [4]. A V-4531 cavity, operating in the E_{102} modes, was used and the powder samples were placed in a 3 mm bore quartz tube located at the cavity centre; slots in the front face of the cavity allowed direct irradiation of the powder *in situ*. A Philips 90 watt mercury lamp provided the source of ultraviolet (UV) radiation with, when necessary, a copper sulphate solution filter to absorb the infrared (IR) component of the lamp's output; a lens focused the beam on to the optical window of the cavity. The continuous flow liquid helium cryostat enabled the spectra to be recorded at temperatures between 300 and 4.2 K.

2.3. Computer simulation

A computer program, similar to that used by Thorp and Hutton [5] in ESR studies of glasses and glass ceramics, was used in this work to simulate spectra from rutile powder samples. The program applies to $S = 1/2, I = 0$ systems, with cubic, axial or orthorhombic symmetry, and can incorporate either Gaussian or Lorentzian line broadening fucntions. The basic steps of the program are as follows.

Firstly, random orientation is represented by calculating g-values at each of 20 000 different orientations, equally incremented over the whole solid angle, from

$$g = (g_1^2 \sin^2\theta \sin^2\phi + g_2^2 \sin^2\theta \cos^2\phi + g_3^2 \cos^2\theta)^{1/2} \quad (1)$$

where g_1, g_2 and g_3 are the g-values along the principle crystal axes, and θ and ϕ define the orientation with respect to the magnetic field.

Next, the corresponding resonance field value for each element is found from

$$H = \frac{h\nu}{g\beta}. \quad (2)$$

A histogram is then created of the number of elements with resonance fields occurring in each cell of a magnetic field array, $H_1 \rightarrow H_n$, incremented in 0.5 gauss intervals. This leads to the full lines in the upper traces of Fig. 1. The effect of crystallite line broadening is introduced by multiplying the value in each cell of the magnetic field

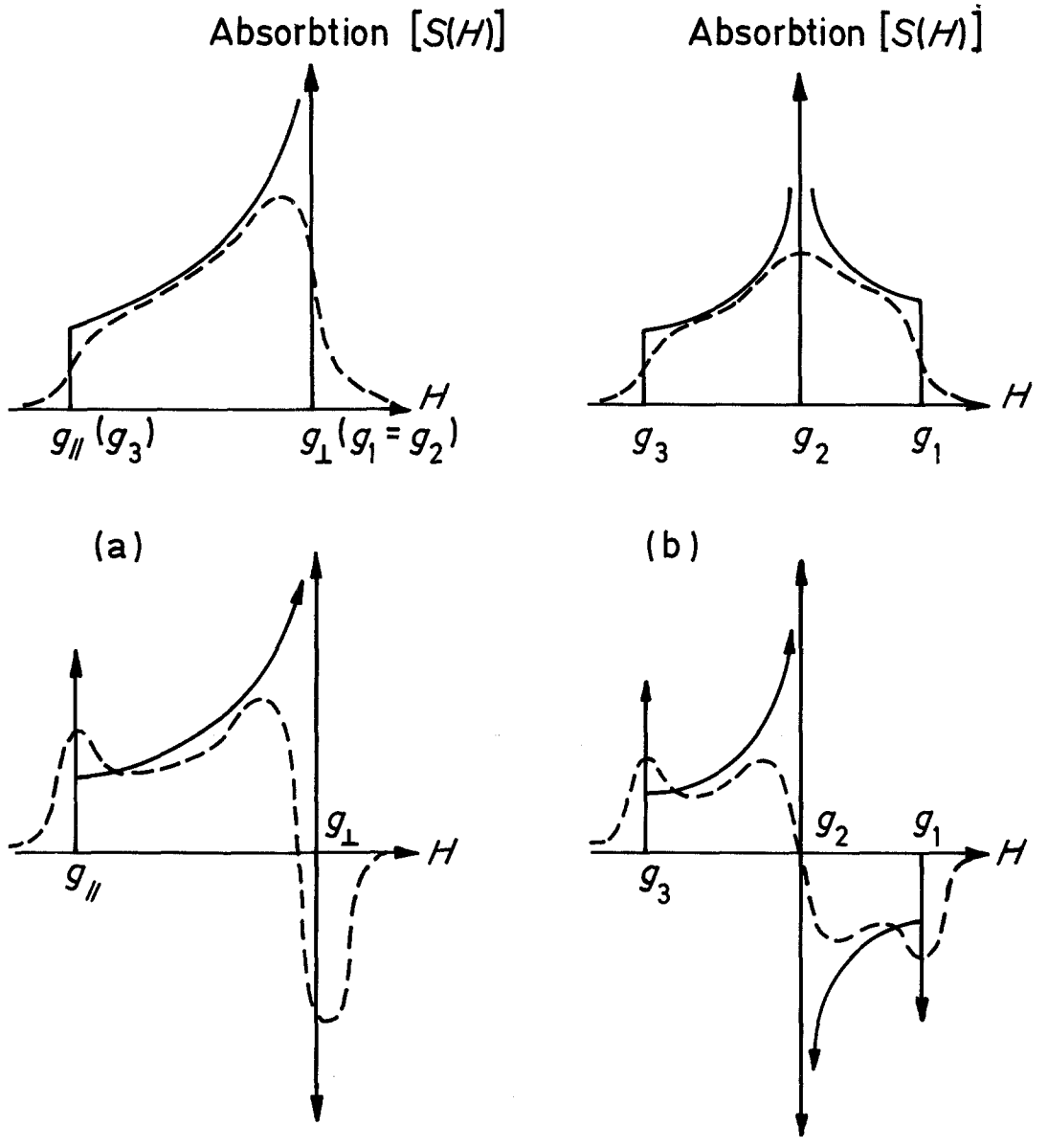

Figure 1 Powder spectra from sites with (a) axial symmetry (b) orthorhombic symmetry. Upper traces are absorption spectrum. Lower traces are the first derivatives of the spectrum. Full lines are idealized spectra with δ function absorption by individual crystallites. Dotted lines are "real" spectra, i.e. the effect of crystallite line broadening.

array by an appropriate normalized single crystal lineshape function, giving the dashed lines in the upper traces of Fig. 1. The lineshape function can be either Gaussian, to simulate spin–spin broadening,

$$G(H_0 - H) = \frac{1}{(2\pi)^{1/2}} \frac{1}{\sigma_G} \exp\left(\frac{-(H_0 - H)^2}{2(\sigma_G)^2}\right) \quad (3)$$

where $2\sigma_G$ is the width at half-height. Alternatively, a Lorentzian function may be used, representing spin–lattice broadening,

$$F(H_0 - H) = \frac{1}{\pi} \frac{2/\sigma_L}{(2/\sigma_L)^2 (H_0 - H) + 1} \quad (4)$$

where σ_L is the width at half-height. The final step is to compute the first derivative of the absorption lineshape in order to give a direct comparison with as-recorded experimental spectra.

While this computation can be a very useful tool under ideal conditions, it should be realized that it includes some assumption which will often preclude an exact simulation of a real spectrum. In practice it is unlikely that the true broadening

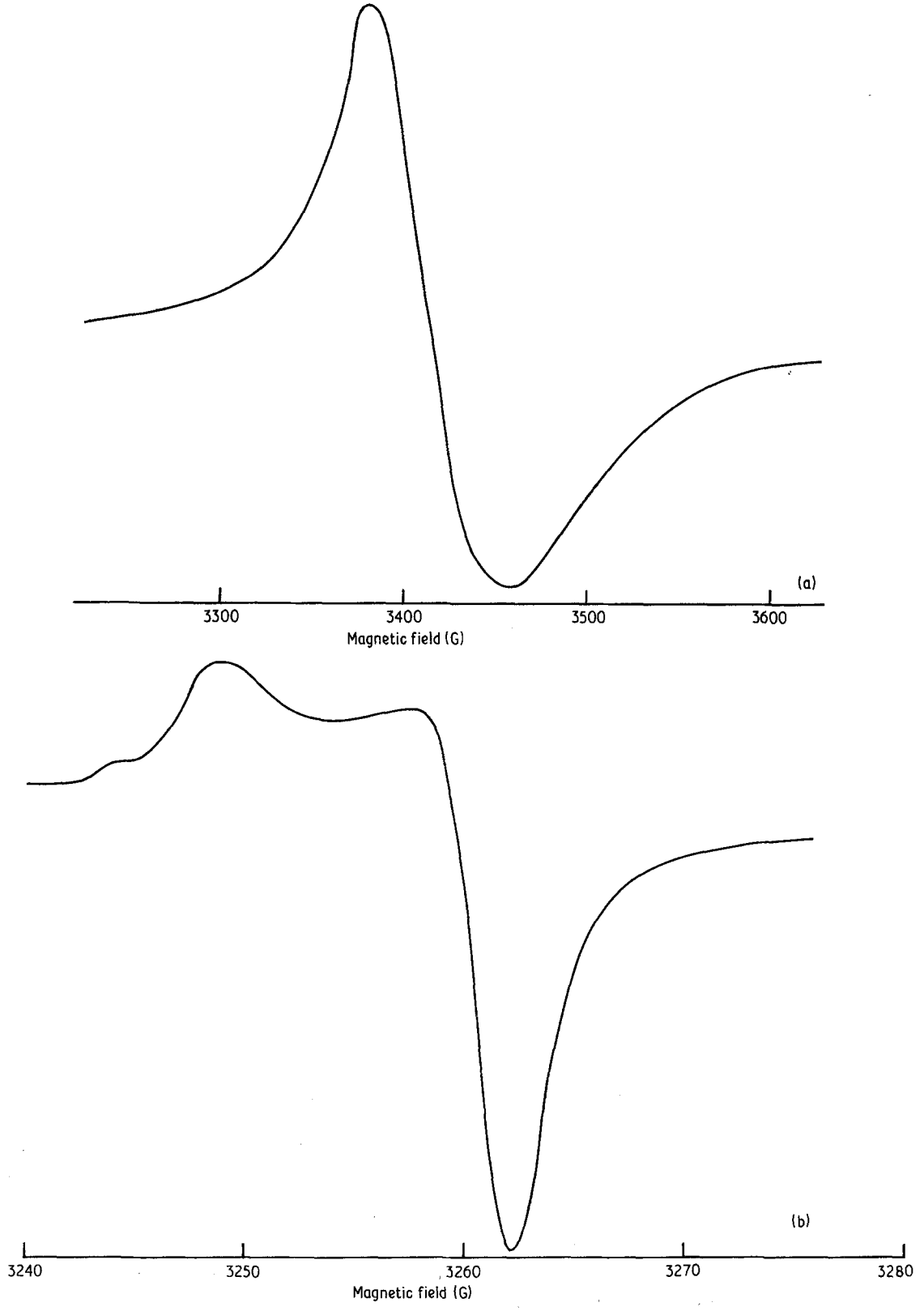

Figure 2 Experimental powder spectra: (a) signal P, recorded at 4.2 K, $\nu = 9.331$ GHz (powder G) (b) powder spectrum Q, created by UV irradiation at 4.2 K, $\nu = 9.166$ GHz.

function will be either completely Gaussian or completely Lorentzian, but rather a combination of the two. Similarly, it is also unlikely that the recorded spectrum will be a true first derivative of the absorption line. Furthermore, it is possible that the recorded spectrum may not be representative of the true lineshape, due to such effects as overlapping with other signals or baseline drift. For these reasons the best-fit simulated pattern usually consists of a compromise between reproduction of different features of the true spectrum.

3. Results

3.1. Initial characterization

Initial measurements of the 9 GHz ESR powder spectra were made at room temperature and the main features noted were as follows. Sample A gave a broad asymmetric line at $g \sim 2.10$. This signal was not detected in sample B. Both powders C and D gave asymmetric lines at $g \sim 2.07$, of similar intensity in each sample. In addition, sample C also had a small, near-symmetric line at $g \sim 2.00$, which was not present in sample D. No signals were detected in either sample E or sample F. Reference to Table I suggests that the signals at $g \sim 2.10$ and $g \sim 2.00$ in samples A and C, respectively, may be associated with intrinsic defects which are removed by annealing in an oxidizing ambient at 600° C. The signal at $g = 2.07$, which was unaffected by oxidation, was only found in samples containing 3.28% Al_2O_3. Since this level is greater than the maximum solubility of aluminium in rutile (Slepetys [6]) it is possible that this signal may represent the presence of a new phase, such as Al_2TiO_5. It is interesting to note in this connection that Al_2TiO_5 has in fact been identified by X-ray diffraction in similar samples, (Egerton [7]).

Measurements at 4.2 K with the Varian spectrometer showed the presence of two weak asymmetric lines in all the powder samples, at magnetic fields corresponding to $g \sim 4.1$ and $g \sim 2.0$. In addition sample E also gave rise to a weak isotropic line at $g \sim 1.89$. The only powder to produce a signal of sufficient intensity to allow accurate recording of the lineshape for computer simulation was sample G, which had been reduced in hydrogen. This signal, spectrum *P*, is shown in Fig. 2a. The line is broad (about 80 gauss from positive to negative peaks) and slightly anisotropic, with a zero-crossing magnetic field corresponding to $g \sim 1.955$, i.e. similar to the value reported by Iyengar [1], also in H_2-reduced rutile powder.

3.2. UV induced spectra

Ultraviolet irradiation of the powder samples at 4.2 K had no observable effect on the intensities of the signals reported in the previous section, but caused the appearance of a new signal, spectrum

TABLE III ESR parameters of defects in non-stoichiometric rutile

g_{110}	g_{110}	g_{001}	Remarks	Interpretation	Reference
$g_x = 1.974$	$g_y = 1.977$	$g_z = 1.941$	x, y are 19° from ⟨110⟩ in (001) plane	Interstitial Ti^{3+} Interstitial H^+	[8] [9]
1.965	1.965	1.935		F centre	[10]
1.975	1.978	1.953		Subst. Ti^{3+}	[11]
1.9777	1.9743	1.9436	seen in Pt-doped crystal	Subst. Ti^{3+}	[12]
$g_x = 1.916$	$g_y = 1.952$	1.814	vacuum-reduced Al-doped	Ti^{3+}–Al^{3+}–Al^{3+}	[13]
$g_x = 1.850$	$g_y = 1.885$	1.932	vacuum-reduced Al-doped	Ti^{3+}–Ti^{3+} –Al^{3+}–Al^{3+}	[13]
$g_x = 1.962$	$g_y = 2.040$	1.709	vacuum-reduced Al-doped	Ti^{3+}–Ti^{3+} –Al^{3+}–Al^{3+}	[13]
1.965	1.965	1.965	vacuum-reduced Al-doped	F centre	[13]
$g_x = 1.885$	$g_y = 1.915$	1.825	vacuum-reduced Al-doped		[13]
1.980	1.978	1.956	Tr < 450° C	F centre trivalent impurity	[14]
1.923	1.896	1.793	Al-doped	Ti^{3+} with nearby Al	[14]
1.923	1.912	1.828	Al-doped		[14]
1.924	1.957	1.78	Reduced in H_2		[14]
1.985	1.989	1.932			[14]
1.964	1.971	1.971			[14]
1.964	1.994	1.928	Ti-doped		[14]
1.954	1.979	1.950	Ti-doped		[14]

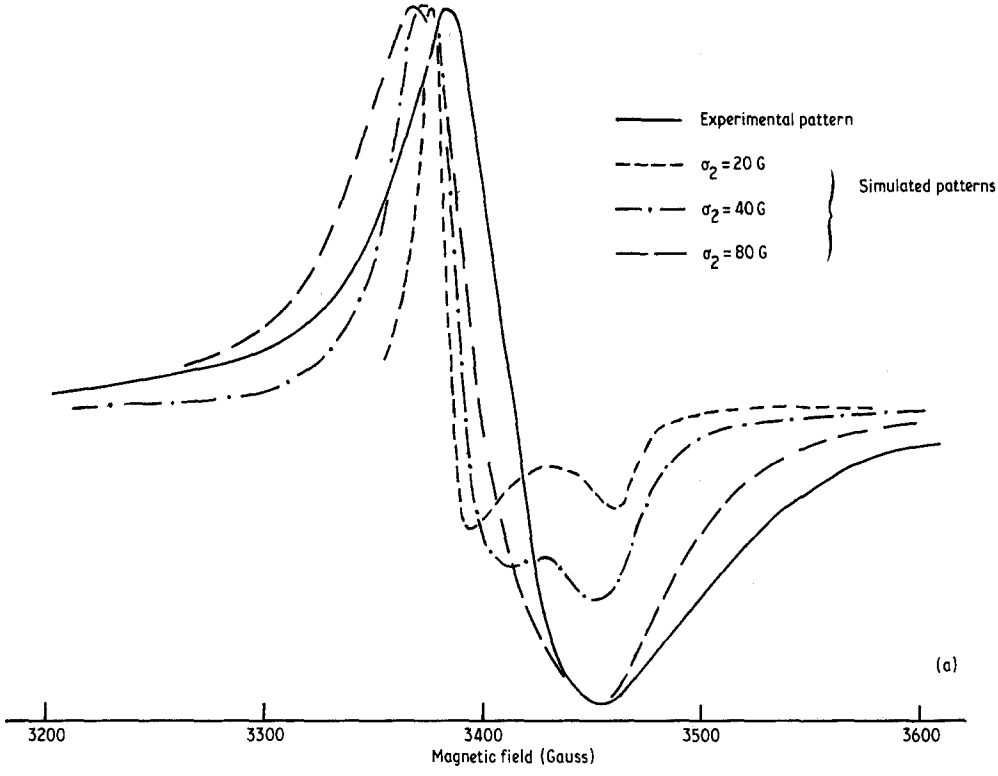

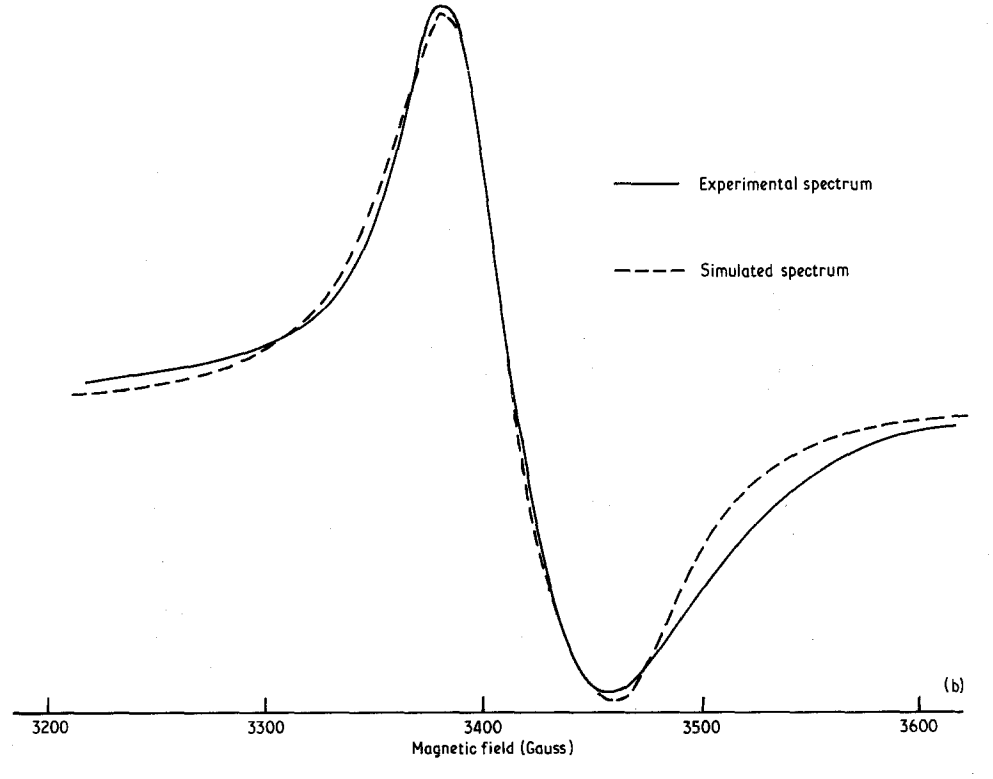

Figure 3 (a) Comparison of experimental powder spectrum P with simulated spectra representing $g_1 = g_2 = 1.9714$, $g_3 = 1.9280$ and varying broadening functions; $\nu = 9.331$ GHz. (b) Comparison of experimental powder spectrum P with best-fit simulated spectrum: $g_1 = g_2 = 1.962$, $g_3 = 1.923$, $\sigma_2 = 80$ G, $\nu = 9.331$ GHz.

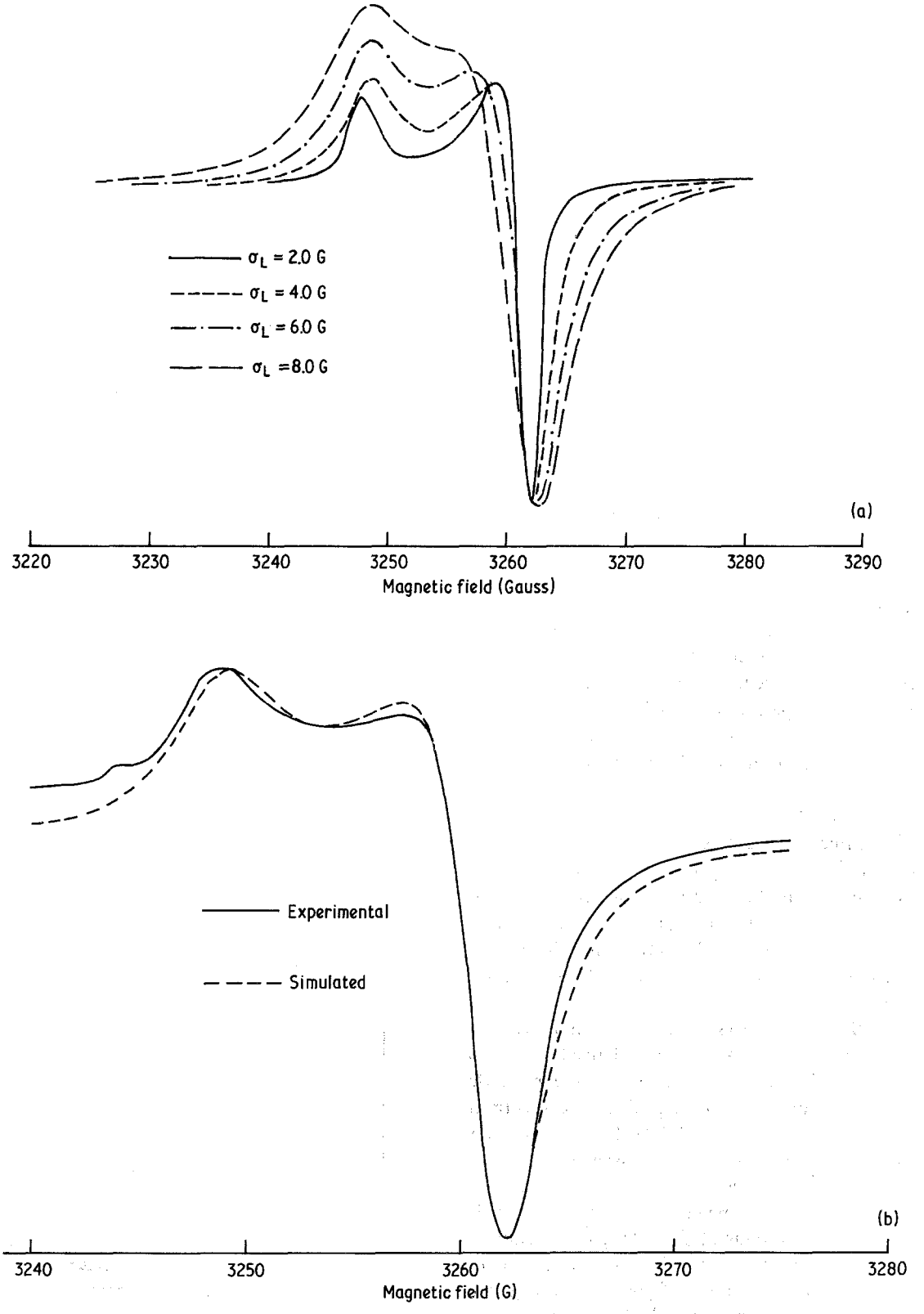

Figure 4 (a) Simulated powder spectra for $g_1 = g_2 = 2.0074$, $g_3 = 2.0155$, showing the effect on lineshape of varying the broadening function; $\nu = 9.166$ GHz. (b) Comparison of experimental powder spectrum Q, with best-fit simulated spectrum $g_1 = g_2 = 2.0077$, $g_3 = 2.0153$, $g_2 = 5.5$ G; $\nu = 9.166$ GHz.

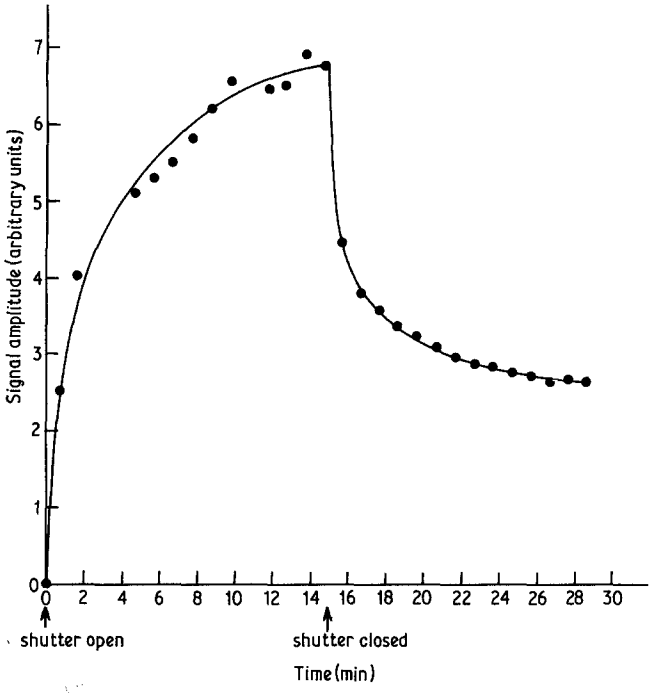

Figure 5 Variation of amplitude of signal Q with time, during and after UV irradiation at 4.2 K (powder D).

Q, at $g \sim 2.01$. The same signal, a trace of which is shown in Fig. 2b, was detected in all seven powder samples, but its intensity varied considerably. Although no accurate spin calibration measurements were performed, qualitative comparisons suggested that the intensity was greater in samples which had received the oxidizing heat treatment.

4. Discussion

The principal features of the powder spectra observed, that is the spectrum P observed at 4.2 K in sample G and the spectrum Q which was seen in all the powders after UV irradiation at 4.2 K, were analysed by computer simulation procedures in an attempt to derive some structural information about them.

Initial attempts to simulate spectrum P assumed axial symmetry (because of the relative lack of features, cf. Fig. 1), with $g_{\|}$ defined by the magnetic field value of the positive peak in the spectrum ($g_{\|} = 1.9714$ and $g_{\perp} = 1.9280$). Fig. 3a compares spectra simulated with these g-values, for three different magnitudes of Lorentzian broadening function with the experimental spectrum. This shows that a σ_L value of about 80 gauss is required to produce the same lack of features, while retaining the appropriate ratio of positive and negative peak heights. Gaussian broadening functions gave lines that were too symmetrical. Slight adjustments to g-parameters to give $g_{\|} = 1.962$ and

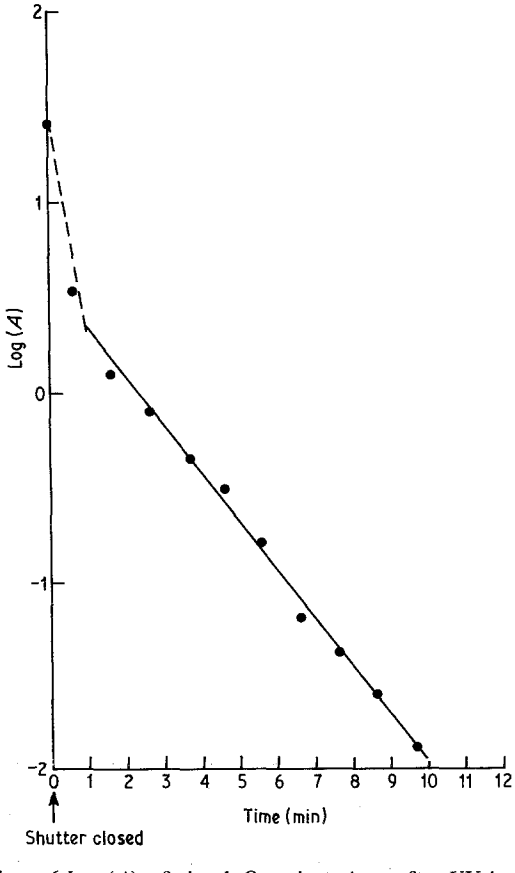

Figure 6 Log(A) of signal Q against time, after UV irradiation at 4.2 K (powder D).

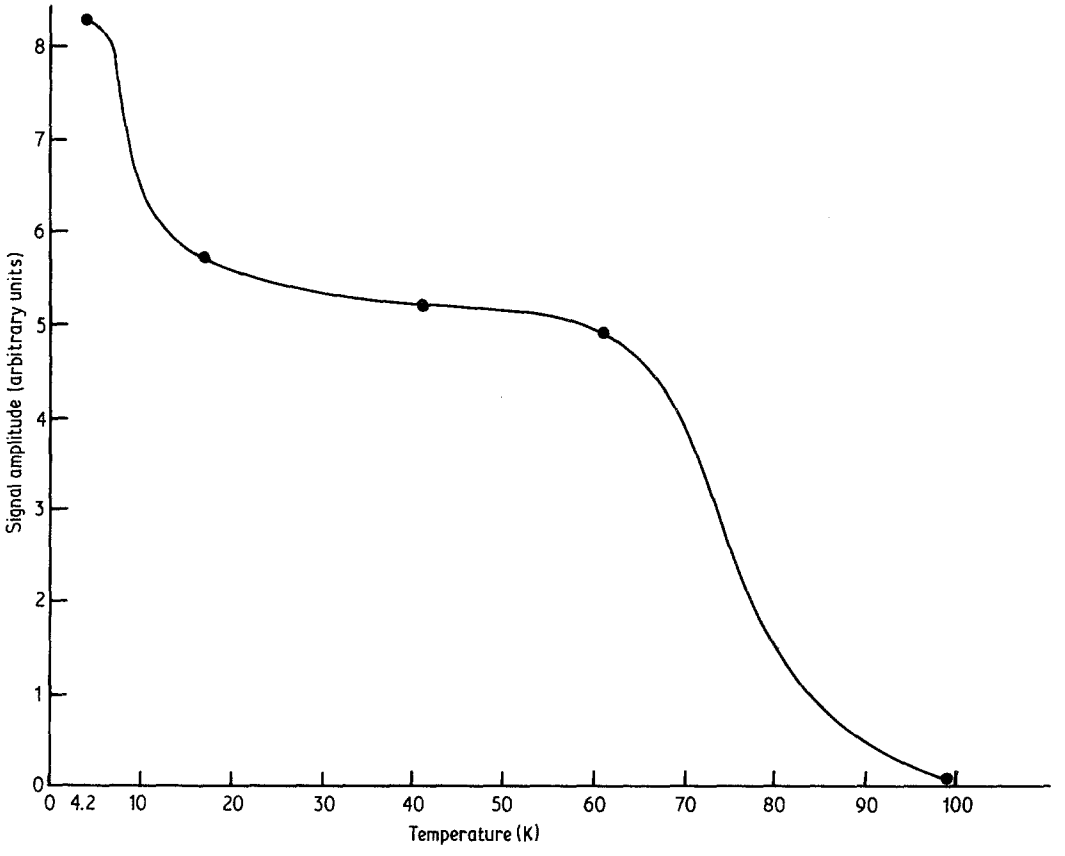

Figure 7 Effect of isochronal annealing on the amplitude of signal Q, following UV irradiation at 4.2 K (powder E).

$g_\perp = 1.923$ yielded the simulated pattern shown in Fig. 3b. The peaks and zero-crossing fields of the two patterns coincide within experimental limits, as does the rate of rise of the positive peak, though the rate of fall of the negative peak is less well matched. Introduction of a small degree of orthorhombic distortion produced no improvement in alignment and therefore Fig. 3b represents the best fit simulated spectrum, within the limitations of the program. Thus, it appears that spectrum P may be described by $g_1 = g_2 = 1.962$ and $g_3 = 1.923$ together with a Lorentzian line broadening function, and $\sigma_L = 80$ gauss. Reference to Table III, which lists known ESR parameters from non-stoichiometric rutile single crystals, shows that the parameters of spectrum P are similar to several others which have been interpreted as being due to intrinsic defects, either F centres or interstitial Ti^{3+}.

The first simulations of spectrum Q compared Lorentzian and Gaussian broadening functions with varying linewidths using axial symmetry. As with spectrum P, it was found that a Gaussian function was inappropriate, being unable to reproduce the peak height ratios while retaining the correct half-height widths. Better progress was made with the Lorentzian function and Fig. 4a depicts lineshapes for four different values of σ_L, with $g_1 = g_2 = 2.0074$ and $g_3 = 2.0155$. A value of $\sigma_L = 6.0$ gauss gives the best reproduction of the shape of the shoulder at about 3258 gauss. Further small adjustments in the parameters gave the best fit simulated pattern, as shown in Fig. 4b, with $g_1 = g_2 = 2.0077$, $g_3 = 2.0153$ and $\sigma_L = 5.5$ gauss. Thus the spectrum appears to be unlike any other reported from ESR measurements on rutile powders. Moreover, the parameters cannot be matched with any of the data [4] for centres in UV-irradiated single crystals. It is thought that since the g-values are greater than the free electron value, spectrum Q may represent a trapped hole similar to that described by Zwingel [15].

Further evidence for this interpretation was gained from isochronal annealing and isothermal decay measurements. Fig. 5 gives the variation of signal amplitude during and after UV irradiation at 4.2 K and shows an exponential growth during irradiation, followed by a rapid fall to about 40% of maximum intensity when irradiation ceases. It

is suggested that this behaviour corresponds to the filling of both hole-trapping and electron-trapping centres during irradiation and then thermal release of electrons from shallow traps followed by their recombination at hole traps, causing the decrease in the number of "Q" centres. The change in slope of the log plot given in Fig. 6 shows that two decay rates are involved and it seems probable that this recombination process is initially monomolecular and that later, as retrapping becomes significant, the kinetics change to bimolecular. Isochronal annealing of signal "Q" between 4 and 100 K (Fig. 7) revealed two temperature regions in which charge transfers occurred, both causing further decreases in the intensity of "Q". The first, at about 10 K, is assumed to correspond to thermal release of electrons from another shallow trapping level and subsequent recombination at "Q" centres. The second, at about 80 K, may either represent a similar process with a deeper electron trap or the direct thermal release of trapped holes.

Acknowledgements

It is a pleasure to acknowledge the help received from Dr T. Egerton, Tioxide International Ltd. (Central Laboratories, Stockton-on-Tees) who supplied the powders and mass-spectrographic analyses.

One of us (SWH) also wishes to thank the Science and Engineering Research Council for the award of a postgraduate studentship.

References

1. R. D. IYENGAR, *J. Colloid Interface Sci.* **35** (1971) 424.
2. M. PRIMET, *J. Chim. Phys.* **67** (1970) 1627.
3. H. S. EGGLESTON and J. S. THORP, *J. Mater. Sci.* **16** (1981) 537.
4. S. W. HODGSKISS, PhD thesis, University of Durham (1981).
5. J. S. THORP and W. HUTTON, *J. Phys. Chem. Solids* **42** (1981) 843.
6. R. A. SLEPETYS, *J. Phys. Chem.* **73** (1969) 2157.
7. T. EGERTON, private communication (1982).
8. P. F. CHESTER, *J. App. Phys.* **32** (1961) 866.
9. L. N. SHEN, *Phys. Rev. B* **10** (1974) 1823.
10. V. N. BOGOMOLOV, *Sov. Phys. Solid State* **9** (1968) 2647.
11. H. J. GERRITSEN, *Phys. Rev.* **125** (1962) 1853.
12. G. V. CHANDRASHEKHAR, *J. Electrochem. Soc.* **123** (1976) 392.
13. J. KERSSEN, *Physica* **69** (1973) 535.
14. P. F. CHESTER, CERL Report RD/L/R (1964) p. 1267.
15. D. ZWINGEL, *Solid State Commun.* **20** (1976) 397.

Received 11 November
and accepted 20 December 1982